

## Discovery of Nonsteroidal 17 $\beta$ -Hydroxysteroid Dehydrogenase 1 Inhibitors by Pharmacophore-Based Screening of Virtual Compound Libraries

Daniela Schuster,<sup>||†</sup> Lyubomir G. Nashev,<sup>||‡</sup> Johannes Kirchmair,<sup>†</sup> Christian Laggner,<sup>†</sup> Gerhard Wolber,<sup>§</sup> Thierry Langer,<sup>\*,†,§</sup> and Alex Odermatt<sup>\*,‡</sup>

Computer-Aided Molecular Design Group, Department of Pharmaceutical Chemistry, University of Innsbruck, Innrain 52c, A-6020 Innsbruck, Austria, and Center of Molecular Biosciences Innsbruck—CMBI, Peter-Mayr-Strasse 1a, A-6020 Innsbruck, Austria, Molecular and Systems Toxicology, Department of Pharmaceutical Sciences, University of Basel, Klingelbergstrasse 50, CH-4056 Basel, Switzerland, Inte:Ligand Software-Entwicklungs and Consulting GmbH, Mariahilferstrasse 74B/11, A-1070 Wien, Austria

Received January 23, 2008

17 $\beta$ -Hydroxysteroid dehydrogenase type 1 (17 $\beta$ -HSD1) plays a pivotal role in the local synthesis of the most potent estrogen estradiol. Its expression is a prognostic marker for the outcome of patients with breast cancer and inhibition of 17 $\beta$ -HSD1 is currently under consideration for breast cancer prevention and treatment. We aimed to identify nonsteroidal 17 $\beta$ -HSD1 inhibitor scaffolds by virtual screening with pharmacophore models built from crystal structures containing steroidal compounds. The most promising model was validated by comparing predicted and experimentally determined inhibitory activities of several flavonoids. Subsequently, a virtual library of nonsteroidal compounds was screened against the 3D pharmacophore. Analysis of 14 selected compounds yielded four that inhibited the activity of human 17 $\beta$ -HSD1 (IC<sub>50</sub> below 50  $\mu$ M). Specificity assessment of identified 17 $\beta$ -HSD1 inhibitors emphasized the importance of including related short-chain dehydrogenase/reductase (SDR) members to analyze off-target effects. Compound **29** displayed at least 10-fold selectivity over the related SDR enzymes tested.

### Introduction

The estrogen receptor (ER)-mediated<sup>a</sup> regulation of gene transcription is dependent on the local availability of the active estrogen estradiol. The ratio of the weak estrogen estrone to its potent metabolite estradiol is regulated by 17 $\beta$ -hydroxysteroid dehydrogenase (17 $\beta$ -HSD) enzymes. Upon irreversible conversion of testosterone to dihydrotestosterone by 5 $\alpha$ -reductase, several 17 $\beta$ -HSD enzymes are also involved in androgen metabolism. Thus, the expression of 17 $\beta$ -HSDs plays a crucial role in balancing the intracellular activity of estrogens and androgens. So far, 14 different enzymes have been assigned to the 17 $\beta$ -HSDs, mainly due to sequence similarity, although for some them (17 $\beta$ -HSD6, -9, and -13) the activity has not been confirmed.<sup>1–4</sup> 17 $\beta$ -HSD1 (EC 1.1.1.62) plays a pivotal role in the local estradiol production in syncytiotrophoblasts of the human placenta, in granulosa cells of the ovary, and in the mammary gland by catalyzing the NADPH-dependent reduction of estrone to estradiol.<sup>5</sup> The conversion of dehydroepiandrosterone (DHEA) into 5-androstene-3 $\beta$ ,17 $\beta$ -diol is also catalyzed by 17 $\beta$ -HSD1, although at a lower rate.<sup>6</sup> An overview of the involvement of 17 $\beta$ -HSDs and other enzymes<sup>7,8</sup> in sex hormone biosynthesis and regulation is given in Scheme 1.

Several recent studies provided evidence for the use of 17 $\beta$ -HSD1 expression levels as a prognostic marker for the overall and disease-free survival of patients with breast cancer.<sup>9–11</sup> 17 $\beta$ -HSD1 is currently considered as a promising target for local inhibition of estradiol biosynthesis in the prevention or treatment of breast cancer in premenopausal women and especially in postmenopausal women, where the local production represents the major source of estradiol. Husen et al. recently reported that treatment with a specific 17 $\beta$ -HSD1 inhibitor significantly decreased the estrogen-dependent growth of xenografts expressing 17 $\beta$ -HSD1 in vivo in mice.<sup>12</sup> In contrast, reduced expression of 17 $\beta$ -HSD2, catalyzing the conversion of estradiol to estrone, has been associated with colon cancer.<sup>13</sup> Thus, 17 $\beta$ -HSD1 inhibitors have to be highly specific to avoid disturbances of 17 $\beta$ -HSD2 and other members of the short-chain dehydrogenase/reductase (SDR) family.<sup>14</sup>

Human 17 $\beta$ -HSD1 consists of 327 amino acids with a molecular weight of 34.9 kDa and functions as a homodimeric complex. As with all SDR enzymes, it contains the Rossmann fold for cofactor binding and the highly conserved Tyr-X-X-X-Lys sequence in the ligand binding and enzymatically active region. The core structure consists of the seven-stranded parallel  $\beta$ -sheet surrounded by six parallel  $\alpha$ -helices, three on each side of the  $\beta$ -sheet. Five additional  $\alpha$ -helices are located around the steroid binding domain.<sup>15</sup> 17 $\beta$ -HSD1 has been extensively studied in X-ray crystallography experiments with 15 structures of human 17 $\beta$ -HSD1 in the Protein Data Bank (PDB) (Supporting Information Table S1).<sup>15–24</sup>

The steroid binding pocket of 17 $\beta$ -HSD1 can be divided into three regions. The first region recognizes the steroid phenolic A-ring and contains His221 and Glu282, which could form hydrogen bonds with O3 of the steroid.<sup>15</sup> The second region binds to the central hydrophobic core of the steroid and contributes to the main thermodynamic force favoring the binding of substrates. The third region (catalytic region) surrounds the D-ring and contains Ser142, Tyr155, and Lys159.

\* To whom correspondence should be addressed. Alex Odermatt: Phone: +41 61 267 1530 (A.O.); +43 (512) 507-5252 (T.L.). Fax: +41 61 267 1515 (A.O.); +43 (512) 507-5269 (T.L.). E-mail: Alex.Odermatt@unibas.ch (A.O.); Thierry.Langer@uibk.ac.at (T.L.).

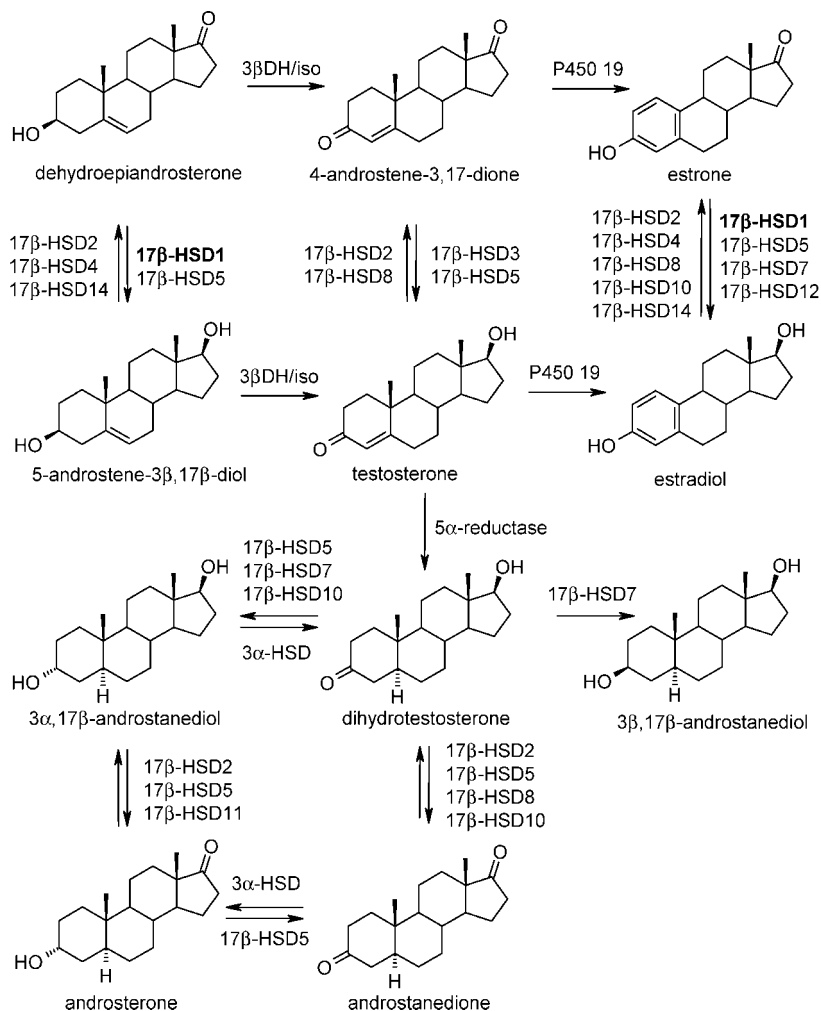
<sup>†</sup> Computer-Aided Molecular Design Group, Department of Pharmaceutical Chemistry, University of Innsbruck, and Center of Molecular Biosciences Innsbruck—CMBI.

<sup>‡</sup> Molecular and Systems Toxicology, Department of Pharmaceutical Sciences, University of Basel.

<sup>§</sup> Inte:Ligand Software-Entwicklungs and Consulting GmbH.

<sup>||</sup> D.S. and L.G.N. contributed equally to this work.

<sup>a</sup> Abbreviations: 11 $\beta$ -HSD, 11 $\beta$ -hydroxysteroid dehydrogenase; 17 $\beta$ -HSD, 17 $\beta$ -hydroxysteroid dehydrogenase; AKR, aldoketo reductase; DHEA, dehydroepiandrosterone; ER, estrogen receptor; HBA, hydrogen bond acceptor; HBD, hydrogen bond donor; SDR, short-chain dehydrogenase/reductase; WDI, World Drug Index.

Scheme 1. Role of 17 $\beta$ -HSD1 in Sex Hormone Biosynthesis<sup>a</sup>

<sup>a</sup> Abbreviations used: 3 $\beta$ DH/iso, 3 $\beta$ -dehydrogenase/isomerase; P450 19, cytochrome P450 19 (also known as aromatase); 3 $\alpha$ -HSD, 3 $\alpha$ -hydroxysteroid dehydrogenase.

The reduction reaction involves a proton and a hydride, which are transferred to the estrone molecule, whereby Tyr155 is the likely candidate to donate a proton to O17. Ser142 should be able to share its proton with Tyr155, therefore stabilizing the nonprotonated state of the Tyr residue. The  $\alpha$ -face of the steroid is accessible to the nicotinamide to facilitate hydride transfer. The major role of Lys159 could be the stabilization of the dinucleotide NADP<sup>+</sup> through the interaction with the nicotinamide ribose.<sup>15</sup>

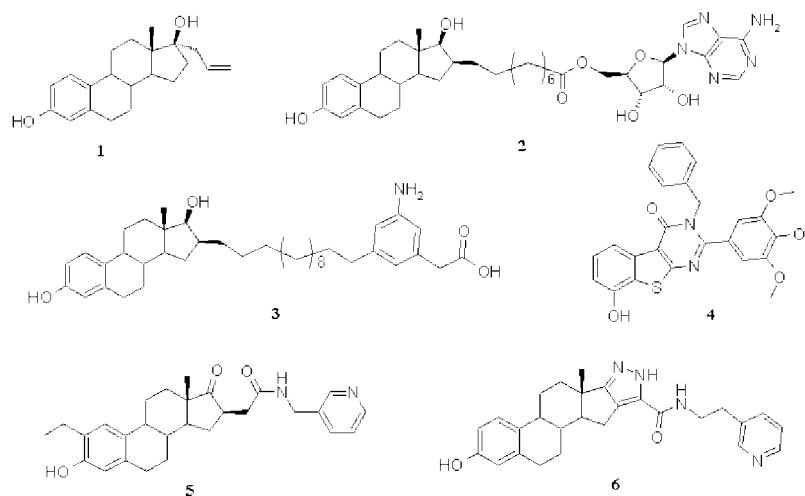
17 $\beta$ -HSD1 shows a clear preference for estrogen substrates. Because both estrogens and androgens (with C19) have 3- and 17-hydroxyl or ketone groups, the critical residues that are expected to determine specificity for the estrogenic substrates must lie within the hydrophobic binding region. For dihydrotestosterone and dehydroepiandrosterone, crystallization experiments confirmed this hypothesis by showing that the C19 methyl group causes a shift of the substrate compounds away from NADP<sup>+</sup>, resulting in a lower  $k_{cat}$  value.<sup>18</sup> Especially the rigidity of the fork-like side chain Leu149 forced the androgens to occupy a slightly different site than estradiol in the PDB complex 1fdt. Subsequently, the important van der Waals contacts between Phe259 and the ligand loosened, implementing a loss of favorable interaction and thus decreasing the binding affinity. Indeed, the  $K_m$  value for dehydroepiandrosterone is

more than 1000-fold greater than that for estrone, and the  $K_m$  for dihydrotestosterone is about 10-fold greater than that for estradiol.<sup>18</sup>

Basically, 17 $\beta$ -HSD1 can be inhibited at several sites, including the substrate binding pocket and the cofactor binding region with the Rossmann fold.<sup>25</sup> Brown et al. evaluated synthetic gossypol derivatives for 17 $\beta$ -HSD1 inhibitory activity and confirmed in *in vitro* and *in silico* studies that gossylic lactone and gossylic iminolactone compete with NADPH for its binding site at the Rossmann fold.<sup>25</sup>

Another class of inhibitors, mostly steroidal compounds, was shown to compete with the natural substrate for its binding site. Both reversible and irreversible inhibitors are known that occupy the active site of the enzyme.<sup>26,27</sup> Extensive medicinal chemistry analyses of estrogen derivatives revealed a clear picture of favorable and unfavorable substitution sites and substitutions (Supporting Information Table S2).<sup>21,28–34</sup>

A third class of inhibitors consists of so-called hybrid compounds that combine moieties from NAD(P)H and estradiol analogs. These compounds often consist of a steroidal core and more or less extended side chains at positions 16 or 17 that protrude into the NADPH binding site. Several highly efficient 17 $\beta$ -HSD1 inhibitors belong to this class, e.g., compound **2** (EM-1745, IC<sub>50</sub> = 52 nM, K<sub>i</sub> = 3.0 nM), which has been cocrystallized with 17 $\beta$ -HSD 1 (1i5r in the PDB)<sup>21</sup> or compound

Chart 1.  $17\beta$ -HSD1 Inhibitors

**5** ( $IC_{50} = 27$  nM).<sup>35</sup> Chart 1 shows examples of  $17\beta$ -HSD1 inhibitors from different chemical classes.<sup>21,26,31,35–37</sup>

The major disadvantage of steroidal inhibitors and natural phytoestrogen compounds, including flavonoids, is that they generally have unfavorable ADMET characteristics and low specificity due to cross-reactivity with other steroid metabolizing enzymes and steroid hormone receptors. Several of the flavonoid compounds, for example, were shown to also inhibit  $11\beta$ -HSD1 or  $17\beta$ -HSD5.<sup>38–40</sup> Moreover, metabolizing enzymes might modify steroidal inhibitors at several positions of their steroid scaffold, leading to potentially bioactive metabolites and possible disturbances of steroid hormone metabolism. Therefore, there is currently a great interest for the identification of novel nonsteroidal  $17\beta$ -HSD1 inhibitors.

Molecular modeling and virtual screening techniques are widely applied in today's drug discovery process.<sup>41</sup> We recently established pharmacophore models for several pharmacological targets including the SDR enzyme  $11\beta$ -hydroxysteroid dehydrogenase type 1 ( $11\beta$ -HSD1).<sup>42</sup> Other models were successfully used for database screening and led to the identification new inhibitors of aromatase,<sup>43</sup> human rhinovirus coat protein,<sup>44</sup> acetylcholinesterase,<sup>45</sup> and cyclooxygenase.<sup>46</sup> Recently, Messinger et al. reported the identification of novel nonsteroidal  $17\beta$ -HSD1 inhibitors belonging to the pyrimidinone class by applying docking methods.<sup>37</sup> Another group established a 3D QSAR model for thieno[2,3-*d*]pyrimidin-4(3*H*)-one derivatives to guide future structural modifications of this compound class in order to improve their  $17\beta$ -HSD1 inhibitory activity.<sup>47</sup> However, to the best of our knowledge, no pharmacophore model for  $17\beta$ -HSD1 has been established yet. Therefore, we aimed to (i) elucidate pharmacophore models for  $17\beta$ -HSD1 inhibitors according to their binding mode, (ii) use the developed models for activity rationalization of known and newly identified  $17\beta$ -HSD1 flavonoid inhibitors, and (iii) employ the best models for rapid virtual screening in order to find new actives. The actual challenge of this project was that only X-ray crystal complexes containing steroidal inhibitors were available for pharmacophore modeling. On the basis of these data, we aimed to find nonsteroidal inhibitors.

## Results and Discussion

**Structure-Based Pharmacophore Models for Competitive  $17\beta$ -HSD1 Inhibitors.** For fully automated structure-based pharmacophore model generation, LigandScout 2.0, was used.<sup>48,49</sup> Model validation and database searches were run in the Catalyst

program version 4.11.<sup>50</sup> As a starting point for inhibitor modeling, two cocrystallization complexes of  $17\beta$ -HSD1 together with the cofactor  $NADP^+$  and an inhibitor were chosen according to their inhibition site, respectively. The first model representing reversible competitive inhibition was based on the crystal structure of the equestrian estrogen equilin bound to  $17\beta$ -HSD1 (PDB entry 1equ). The second model was derived from the PDB structure 1i5r, where compound **2**, so-called hybrid inhibitor that occupies the steroid as well as the cofactor binding site, was cocrystallized with the enzyme.

**1equ Model.** The initial LigandScout model derived from 1equ represents well all essential ligand–protein interactions described in literature (Figure 1).

The determined interactions were also consistent with binding analysis using the SPROUT program.<sup>51</sup> The final model consisted of three hydrophobic features, one HBD pointing toward His221 and one HBA interacting with Ser142. Fourteen exclusion volume spheres represent amino acid residues and parts of the cofactor flanking the substrate binding pocket. The model was validated by screening a test set (compounds S1–S9, Supporting Information Chart S1)<sup>28,31,52</sup> employing the fast flexible search algorithm of Catalyst. Out of nine steroidal  $17\beta$ -HSD1 inhibitors sharing a comparable binding mode to equilin, all were recognized by the 1equ model. Generally, a model can be validated by examining its World Drug Index (WDI)<sup>53</sup> hitlist for compounds with similar or totally different biological activity. Furthermore, the overall number of hits from the WDI gives an idea of a model's restrictivity. An in-depth description of the WDI is given in the Experimental Section. WDI screening using the 1equ-based model returned 1968 (3.1%) hits. The results of these screening experiments showed that the model was an excellent tool for finding steroidal compounds with  $17\beta$ -HSD1 inhibitory activity. However, the large number of hits from the WDI revealed that this model was rather suitable as a general screening tool where many false positive hits are to be expected.

**1i5r Model.** The second structure-based LigandScout model was based on the cocrystallization complex of  $17\beta$ -HSD1 with compound **2** ( $IC_{50}$  value of 52 nM, PDB complex 1i5r). This complex represents the binding mode of a hybrid compound consisting of a steroidal part and an adenosine, linked by an alkyl chain. For this particular binding mode, very few but potent inhibitors have been reported. Generally, LigandScout includes all chemical interactions that can be formed between the ligand and the protein (electrostatic and hydrophobic contacts) into the



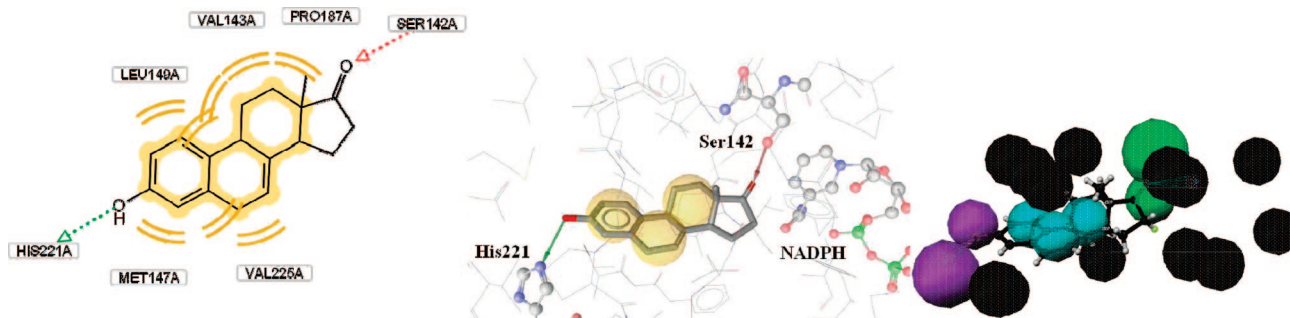


**Figure 1.** 2D and 3D depiction of the interactions of equilin with the 17 $\beta$ -HSD1 binding site as determined by LigandScout (left and center) and Catalyst model (right) for competitive 17 $\beta$ -HSD1 inhibitors based on the PDB entry 1equ. Chemical features are color-coded. LigandScout: green arrows, hydrogen bond donors; red arrows, hydrogen bond acceptors; yellow, hydrophobic regions. Catalyst: magenta, hydrogen bond donors; green, hydrogen bond acceptors; cyan, hydrophobic; black, exclusion volume spheres. For a clearer depiction of the 3D interactions of equilin with the enzyme, no exclusion volume spheres are shown in the LigandScout model.

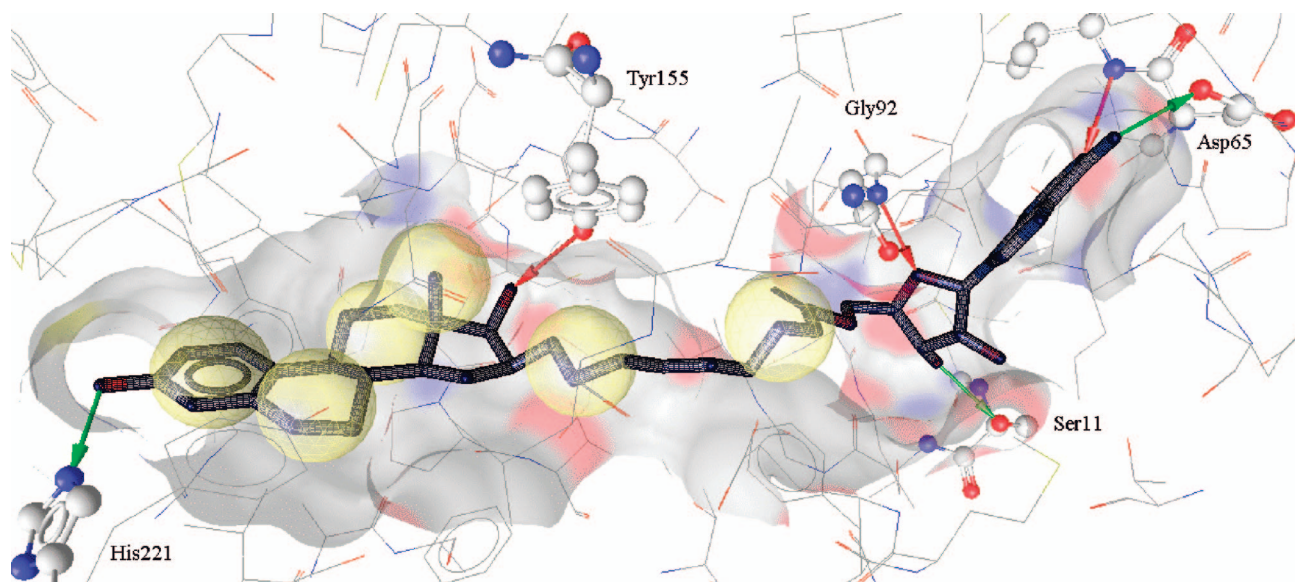


**Figure 2.** LigandScout model after feature reduction for Catalyst compatibility representing the hybrid 17 $\beta$ -HSD1 inhibitor binding mode (1i5r). The hydrophobic feature indicated on the 16-methyl group was not part of the Catalyst model. Exclusion volumes spheres are present in the model but not depicted for clearer visualization. Chemical features are color-coded: green arrows, hydrogen bond donors; red arrows, hydrogen bond acceptors; yellow, hydrophobic regions.

generated pharmacophore models. However, such models can not be directly used in Catalyst because the software can only handle one feature per location. Additionally, hydrophobic spheres are placed on fewer locations than LigandScout indications are present. To generate a Catalyst-compatible pharmacophore model, the model had to be adapted: multiple features (e.g., bifurcated hydrogen bonds) and hydrophobic features not recognized by Catalyst were removed from the initial model. This can either be performed by LigandScout itself ("Create Simplified Pharmacophore (Catalyst)") or manually by the user. Modification of the 1i5r-based model led to a Catalyst-compatible pharmacophore model consisting of five hydrophobic features (three from the steroidal part and two from the alkane chain linker), two HBDs pointing toward His221 (steroidal part) and toward Asp65 (adenosine part), three HBAs toward Tyr155 (steroidal part), Gly92, and Val66 (both adenosine part), two projection points for one HBA (Ser11) and one HBD (Gly9), as well as 10 exclusion volumes spheres representing amino acid residues flanking the ligand binding domain (Figure 2).

This model was able to correctly recognize another hybrid inhibitor, although a structurally closely related one, as being active: compound **S10** (Supporting Information Chart S2). In the WDI, however, no hit was retrieved. One may conclude

that this model is utterly useless for virtual screening employing Catalyst as there are hardly any compounds in commercial libraries that would fit it. Additionally, if there were such compounds, the conformational models for them would have to be exhaustive in order to obtain a fitting conformation. Furthermore, the drug-likeness of eventually fitting compounds might rightfully be questioned. However, the 1i5r model constituted an excellent starting point for a model representing smaller hybrid inhibitors as only introduced in 2005.<sup>35</sup> These compounds do not extend far into the cofactor binding site. They show fewer but similar interactions than compound **S10**. Therefore, we slightly modified the 1i5r model by deleting the adenosine features, merging the hydrophobic features of the alkyl chain linker with each other to one enlarged hydrophobic sphere and replacing the HBA feature of the 17 $\beta$ -hydroxy group by HBA projection points toward Tyr155 and Ser142 (Figure 3).

To evaluate if this 1i5r-reduced model represents a general binding mode of 17 $\beta$ -HSD1 inhibitors, the test set reported in Chart S1 was searched. All inhibitors substituted at position 6 were reported as hits, indicating that this compound class shares a comparable binding mode with the recently reported one (Figure 3). When searching the WDI, 642 compounds (1.0%)

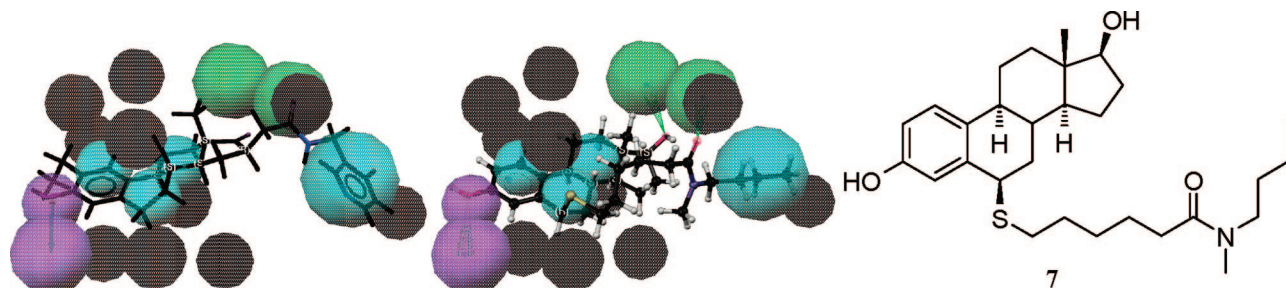


**Figure 3.** The most potent compound of the small hybrid inhibitor series (compound **5**, left) and the potent inhibitor compound **7** ( $IC_{50} = 0.17 \mu M$ , center and right) mapped into the modified hypothesis for  $17\beta$ -HSD1 hybrid inhibitors. Chemical features are color-coded: magenta, hydrogen bond donors; green, hydrogen bond acceptors; cyan, hydrophobic; black, exclusion volume spheres.

were returned as hits. This low number of “random hits” underlines the restrictivity of this model.

**Fitting of Known and Newly Identified  $17\beta$ -HSD1 Inhibitors from the Flavonoid Class.** Several studies suggested that the higher intake of phytoestrogen-rich food contributes to the lower incidence of breast and prostate cancer in the Asian population.<sup>54–56</sup> The major phytoestrogens can be classified as flavones, flavonones, isoflavones, coumestans, and lignans.<sup>57</sup> Structure–activity relationship analyses revealed that the A and C rings of flavones and flavonones mimic the D and C rings of sex steroid molecules. In addition to their potential direct effects on ER, various dietary phytoestrogens can influence ER activation by acting on steroidogenic enzymes, and several of these compounds turned out to be inhibitors of  $17\beta$ -HSD enzymes.<sup>40,58,59</sup>

To validate the  $11\alpha$ -reduced pharmacophore model of  $17\beta$ -HSD1 and to investigate the structure–activity relationships of flavonoids, we applied transiently transfected HEK-293 cells for enzyme activity measurements. These cells are devoid of endogenous expression of steroid hormone-metabolizing enzymes<sup>60–62</sup> and therefore represent a suitable system to investigate the function of individual enzymes.  $17\beta$ -HSD1 activity was determined in cell lysates in the presence of vehicle or  $20 \mu M$  of the respective flavonoid as described previously,<sup>42,61</sup> and  $IC_{50}$  values were determined for compounds inhibiting  $17\beta$ -HSD1 activity by 70% or more (Table 1).

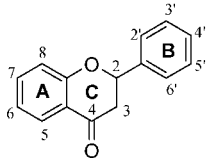
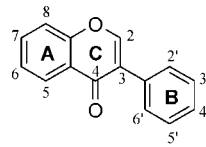
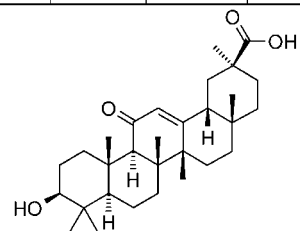
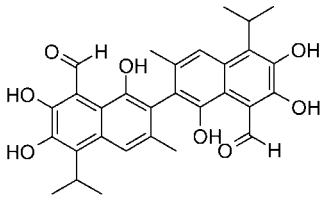
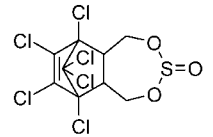
Among the compound **8** (flavanone) derivatives tested, compound **12** was most potent and inhibited  $17\beta$ -HSD1 with an  $IC_{50}$  of  $5 \mu M$ . Compound **13** was less active (44% remaining activity at  $20 \mu M$ ), indicating that the bulkier substituent in the B-ring on C4' or the hydroxyl on C3' negatively affected binding. The hydroxyl groups in the A-ring on C5 and C7 are required because neither compounds **8**, **9**, **10**, nor **11** inhibited  $17\beta$ -HSD1. Among the compound **14** (flavone) derivatives, compound **18**, which has the same hydroxylation pattern as compound **12**, was most potent with an  $IC_{50}$  of  $0.7 \mu M$ , indicating that the double bond between C2 and C3 of the C-ring is favorable for  $17\beta$ -HSD1 inhibition. Compound **18** did not inhibit human  $17\beta$ -HSD2, which is responsible for inactivation of estradiol to estrone. Compound **19**, recently described as an inhibitor of  $17\beta$ -HSD from the fungus *C. lunatus*<sup>63</sup> and which we show here for the first time to be a potent inhibitor of human  $17\beta$ -HSD1, has an additional hydroxyl on C3 in the C-ring and was equally as potent as compound **18**. Unlike compound **18**, compound **19** also was a potent inhibitor of  $17\beta$ -HSD2 with an  $IC_{50}$  of  $0.36 \mu M$ . Compound **20**, with an additional hydroxyl on C5' of the B-ring, was a less active  $17\beta$ -HSD1 inhibitor (65% remaining activity at  $20 \mu M$ ). Our results are in line with a study by Mäkelä et al. reporting that compound **18** but not compound **20** significantly inhibited  $17\beta$ -HSD activity in T-47D

breast cancer cells.<sup>59</sup> The weaker activity of compound **16** (34% remaining activity at  $20 \mu M$ ) compared with compound **18** may be explained by the lack of the 4'-hydroxyl in the B-ring. The 7-hydroxyl of the A-ring seems to be a key functional group because 7-hydroxyflavone was still active. This observation extends an earlier study, suggesting that the C7-hydroxyl on the A-ring of different isoflavones is important for anti- $17\beta$ -HSD activity in placental microsomes compared with inhibition of  $3\beta$ -HSDs.<sup>58</sup> Like compound **8**, the unhydroxylated flavone did not inhibit  $17\beta$ -HSD1. Among the isoflavones, compound **21** most potently inhibited  $17\beta$ -HSD1. In contrast, compound **22** with a bulkier substituent on C4' of the B-ring was less inhibitory (45% remaining activity at  $20 \mu M$ ), and compound **17**, which also was somewhat less active than compound **21**, does not have a hydroxyl on C5 of the A-ring. These results indicate that flavones, flavanones, and isoflavones hydroxylated at position 5 and 7 on the A-ring and position 4' on the B-ring are the most potent inhibitors of  $17\beta$ -HSD1, whereby a bulkier group at position 4' results in a loss of inhibitory potency.

To rationalize the inhibitory activity of the most active flavonoids identified in these experiments, compounds **12**, **18**, and the inactive compound **13** were fitted into our newly developed model based on lequ. However, none of these compounds fitted into the model mapping all features. Therefore, we had a closer look at the binding site and the initial model. This contained more hydrophobic features than a flavonoid could ever fit into. After careful analysis which of the hydrophobic features could be occupied by flavonoids, the remaining hydrophobic sphere (located at the methyl group of equilin) was deleted. Additionally, we assumed that the overall aromatic character of flavonoids has a profound influence on their binding orientation. Accordingly, the hydrophobic function on the aromatic ring of equilin was exchanged for a ring aromatic feature. The most potent inhibitors identified in this study, compounds **12** and **18**, were fitted into the modified pharmacophore model using Catalyst software. Subsequently, the fitting orientation of compound **12** was imported into LigandScout 2.0. Compound **12** fitted nicely into the active site displaying similar interactions with the enzyme as equilin. Excitingly, LigandScout was able to identify interactions that are established between compound **12** and  $17\beta$ -HSD1 that were not present in the model based on equilin: the hydroxyl groups of ring A on C5 and C7 both coordinate the interaction with Glu282 (Figure 4). This highly oriented interaction rationalized the observation that these hydroxyl groups are required for activity of flavonoids. Compound **18** fits into the binding site in a very similar orientation to compound **12**. An additional interaction is observed: the second aromatic ring can also interact with Arg258 (Figure 4).

This difference could explain the higher potency in  $17\beta$ -HSD1 inhibition of compound **18**. Using this approach, also the

**Table 1.** Inhibition of 17 $\beta$ -HSD1 and 17 $\beta$ -HSD2 by Flavonoid Compounds<sup>a</sup>

 Scaffold A (flavanone scaffold)					 Scaffold B (isoflavone scaffold)			
Compound	Scaffold	Ring A	Ring B	Ring C	Inhibition of 17 $\beta$ -HSD1 at 20 $\mu$ M (% activity)	Inhibition of 17 $\beta$ -HSD1 IC <sub>50</sub> ( $\mu$ M), mean $\pm$ SD	Inhibition of 17 $\beta$ -HSD2 at 40 $\mu$ M (% activity)	Inhibition of 17 $\beta$ -HSD2 IC <sub>50</sub> ( $\mu$ M), mean $\pm$ SD
<b>8</b> (flavanone)	A				110 $\pm$ 10	n.d.	70.7 $\pm$ 2.6	n.d.
<b>9</b> (2'-hydroxy-flavanone)	A		2'-OH		95 $\pm$ 18	n.d.	50.7 $\pm$ 0.5	n.d.
<b>10</b> (4'-hydroxy-flavanone)	A		4'-OH		99 $\pm$ 11	n.d.	63.6 $\pm$ 3.5	n.d.
<b>11</b> (6-hydroxy-flavanone)	A	6-OH			102 $\pm$ 6	n.d.	42.5 $\pm$ 1.8	n.d.
<b>12</b> (naringenin)	A	5-OH 7-OH	4'-OH		17.2 $\pm$ 3.9	4.96 $\pm$ 0.33	12.6 $\pm$ 0.8	14.4 $\pm$ 4.5
<b>13</b> (hesperetin)	A	5-OH 7-OH	3'-OH 4'-OMe		44 $\pm$ 5	n.d.	36.4 $\pm$ 1.7	n.d.
<b>14</b> (flavone)	A			$\Delta$ 2,3	94 $\pm$ 10	n.d.	63.9 $\pm$ 0.6	n.d.
<b>15</b> (7-hydroxy-flavone)	A	7-OH		$\Delta$ 2,3	16 $\pm$ 4	5.25 $\pm$ 0.65	23.1 $\pm$ 1.1	> 20
<b>16</b> (chrysin)	A	5-OH 7-OH		$\Delta$ 2,3	34 $\pm$ 3	n.d.	32.8 $\pm$ 5.1	n.d.
<b>17</b> (daidzein)	A	7-OH	4'-OH	$\Delta$ 2,3	35 $\pm$ 5	n.d.	58.3 $\pm$ 6.1	n.d.
<b>18</b> (apigenin)	A	5-OH 7-OH	4'-OH	$\Delta$ 2,3	10 $\pm$ 4	0.71 $\pm$ 0.14	25.2 $\pm$ 0.9	> 20
<b>19</b> (kaempferol)	A	5-OH 7-OH	4'-OH	$\Delta$ 2,3 3-OH	13 $\pm$ 4	1.05 $\pm$ 0.20	4.83 $\pm$ 1.43	0.36 $\pm$ 0.04
<b>20</b> (quercetin)	A	5-OH 7-OH	3'-OH 4'-OH	$\Delta$ 2,3 3-OH	65 $\pm$ 9	n.d.	6.07 $\pm$ 0.74	1.54 $\pm$ 0.22
<b>21</b> (genistein)	B	5-OH 7-OH	4'-OH		17 $\pm$ 4	2.21 $\pm$ 0.33	15.7 $\pm$ 3.0	16.5 $\pm$ 2.7
<b>22</b> (biochanin A)	B	5-OH 7-OH	4'-OMe		45 $\pm$ 3	n.d.	10.1 $\pm$ 0.4	9.90 $\pm$ 1.87
<b>23</b> (glycyrrhetic acid)					53 $\pm$ 6	n.d.	24.5 $\pm$ 2.7	n.d.
<b>24</b> (gossypol)					60 $\pm$ 9	n.d.	64.8 $\pm$ 1.6	n.d.
<b>25</b> (endosulfan)					25 $\pm$ 5	48.25 $\pm$ 11	51.1 $\pm$ 1.3	n.d.

<sup>a</sup> 17 $\beta$ -HSD1 activity was measured by determining the conversion of 200 nM radiolabeled estrone to estradiol in the presence of 500  $\mu$ M NADPH. IC<sub>50</sub> values were determined for several flavonoid compounds that inhibited 17 $\beta$ -HSD1 activity 70% or more at an inhibitor concentration of 20  $\mu$ M. The conversion of estradiol to estrone was measured in the presence of 500  $\mu$ M NADP<sup>+</sup> to assess 17 $\beta$ -HSD2 activity.

diminished inhibitory potency of compound **13** could be hypothesized. Because of the bulkier substitution of the B-ring with a hydroxymethyl group and an additional hydroxyl group, hesperetin can not penetrate into the active site as deep as its

structural relative compound **12**. As a consequence, the stabilizing interactions of the hydroxyl groups of ring A with Glu282 are lost. When the algorithm tries to saturate the hydrogen bonding options that are crucial for ligand orientation, the



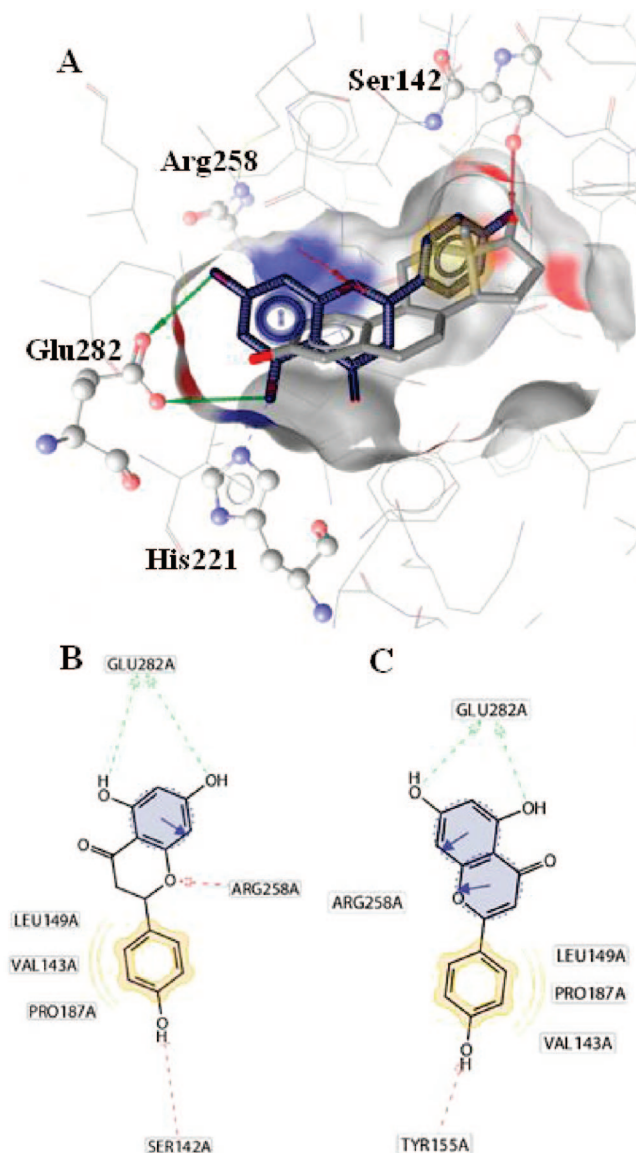


**Figure 4.** Compound **12** fitted into the binding site of  $17\beta$ -HSD1 by pharmacophore-based methods (A). 2D interaction pattern of compound **12** (B) and compound **18** (C).

molecule sterically clashes with Arg258 (Supporting Information Figure S1). The modeling approach could nicely rationalize flavonoid inhibition of  $17\beta$ -HSD1. It also showed that the adaption of structure-based pharmacophore models can be suitable for exploring the binding orientation of chemically unrelated actives. We also evaluated the 1i5r-reduced model by fitting a potent nonsteroidal  $17\beta$ -HSD1 inhibitor reported by Messinger et al., compound **4**, into the pharmacophore.<sup>37</sup> All features except for one hydrophobic were perfectly mapped (Supporting Information Figure S2). We therefore anticipated that the binding mode characterized by our model can also describe binding of nonsteroidal  $17\beta$ -HSD1 inhibitors.

**Virtual Screening for New  $17\beta$ -HSD1 Inhibitors.** To further validate the promising 1i5r-reduced model for its ability to find new active inhibitors, one commercial database and the NCI database were screened for hits. The best flexible search algorithm of Catalyst was used for database mining (Table 2).

Subsequently, hits with high fit values (best fit computed by Catalyst) were docked into the apo binding pocket of 1equ using the docking program GOLD. Overall, GOLD was able to

**Table 2.** Commercially Available Databases Screened with the 1i5r-Reduced Model

database name	database size	no. of hits
NCI	123219	741
Specs	216823	818

correctly reproduce the binding mode of equilin. The collection of NCI and Specs compounds that has been elucidated by screening with the Catalyst pharmacophore query was examined using GOLD. At first the hits were ranked by visual inspection of the docking poses and subsequently ordered by the ChemScore value provided by GOLD.

The final selection of test compounds was performed according to the best fit value, visual inspection of the predicted docking pose, the ChemScore value, and current availability from the compound provider. Chart 2 shows the selected test compounds along with their computed screening properties.

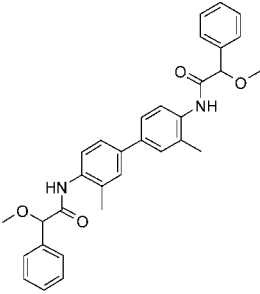
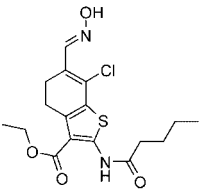
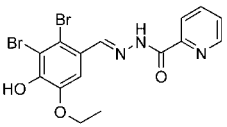
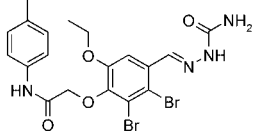
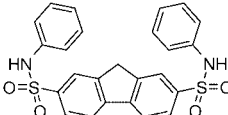
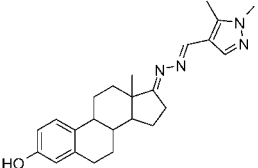
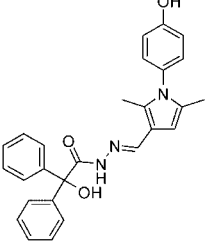
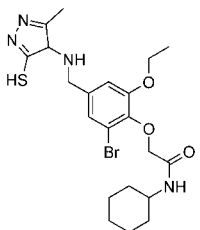
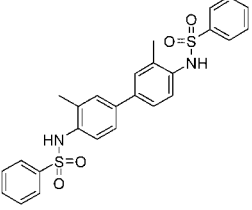
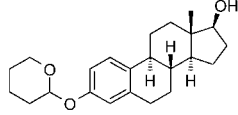
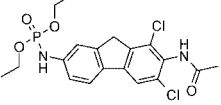
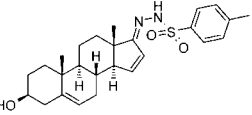
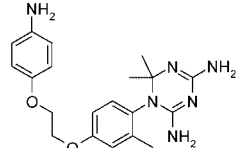
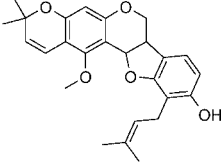
**In Vitro Validation of Compounds Selected after Virtual Screening.** Following virtual screening, 14 compounds were selected and subjected to  $17\beta$ -HSD1 activity assays. Four compounds (28.6%), two with a steroidal and the other two with a nonsteroidal scaffold, inhibited  $17\beta$ -HSD1 with  $IC_{50}$  values below  $50 \mu\text{M}$  (Table 3).

Compound **29** was most potent with an  $IC_{50}$  of  $5.7 \mu\text{M}$ . Thus, despite using a pharmacophore based on steroidal compounds, we succeeded in identifying novel classes of nonsteroidal  $17\beta$ -HSD1 inhibitors that can be used for developing more potent derivatives. Figure 5 shows **29** docked into the  $17\beta$ -HSD1 ligand binding site.

A key issue in the development of therapeutically useful inhibitors is the specificity of a given molecule. Although different members of the SDR family of enzymes share relatively low primary sequence similarity, they share considerable structural similarity. To assess the specificity of the 14 selected compounds, we tested them for potential inhibition of the SDR enzymes  $17\beta$ -HSD2,  $17\beta$ -HSD3, and  $11\beta$ -HSD1 as well as  $17\beta$ -HSD5, a member of the AKR family. Compound **29** showed only weak inhibition of  $17\beta$ -HSD2 and  $11\beta$ -HSD1, with  $IC_{50}$  values clearly higher than  $50 \mu\text{M}$ , while the other enzymes were not affected, suggesting that this compound may serve as a lead for further development. Interestingly, three of the compounds that were selected with the  $17\beta$ -HSD1 pharmacophore inhibited  $11\beta$ -HSD1 with  $IC_{50}$  values below  $20 \mu\text{M}$ , whereas only weak inhibitory effects were observed in measurements of  $17\beta$ -HSD2 and  $17\beta$ -HSD5 activity.  $11\beta$ -HSD1 catalyzes the conversion of the inactive glucocorticoid cortisone to the active form cortisol and plays a pivotal role in the local activation of the glucocorticoid receptor.<sup>64</sup> Thus, interference of a  $17\beta$ -HSD1 inhibitor with  $11\beta$ -HSD1 function might cause adverse effects due to disturbances in glucocorticoid regulation.

The comparison of the effects of the 14 compounds selected with the  $17\beta$ -HSD1 pharmacophore on other  $17\beta$ -HSD enzymes and on  $11\beta$ -HSD1 emphasizes the importance of including several members of the SDR family as well as additional steroid hormone metabolizing enzymes for specificity assessment of a given inhibitor. As an alternative strategy to the biological testing, which is tedious and costly, pharmacophore models of structurally related enzymes can be used as initial filters to eliminate compounds that may cause off-target effects. The availability of pharmacophore models from other members of the SDR family should allow in a first step the elimination of scaffolds with a low degree of selectivity. To test this idea, we

**Chart 2.** Compounds from the NCI and the Specs Database Selected for Biological Testing

 <p style="text-align: center;"><b>26</b> BestFit: 4.06 ChemScore 45.69</p>	 <p style="text-align: center;"><b>27</b> BestFit: 4.40 ChemScore 33.87</p>	 <p style="text-align: center;"><b>28</b> BestFit: 4.64 ChemScore 35.29</p>
 <p style="text-align: center;"><b>29</b> BestFit: 4.00 ChemScore 38.44</p>	 <p style="text-align: center;"><b>30</b> BestFit: 5.00 ChemScore 45.31</p>	 <p style="text-align: center;"><b>31</b> BestFit: 5.14 ChemScore 38.27</p>
 <p style="text-align: center;"><b>32</b> BestFit: 5.04 ChemScore 41.15</p>	 <p style="text-align: center;"><b>33</b> BestFit: 4.08 ChemScore 39.02</p>	 <p style="text-align: center;"><b>34</b> BestFit: 3.99 ChemScore 42.52</p>
 <p style="text-align: center;"><b>35</b> BestFit: 4.33 ChemScore: 39.68</p>	 <p style="text-align: center;"><b>36</b> BestFit: 4.68 ChemScore: 37.83</p>	 <p style="text-align: center;"><b>37</b> BestFit: 4.11 ChemScore: 37.58</p>
 <p style="text-align: center;"><b>38</b> BestFit: 3.92 ChemScore: 30.24</p>	 <p style="text-align: center;"><b>39</b> BestFit: 4.76 ChemScore: 43.09</p>	



**Table 3.** Biological Activities of Compounds Selected after Virtual Screening on Human 17 $\beta$ -HSD1 and Related Enzymes

name	17 $\beta$ -HSD1 % activity at 20 $\mu$ M <sup>a</sup>	17 $\beta$ -HSD1 IC <sub>50</sub> ( $\mu$ M)	17 $\beta$ -HSD2 % activity at 20 $\mu$ M	17 $\beta$ -HSD3 % activity at 20 $\mu$ M	17 $\beta$ -HSD5 % activity at 20 $\mu$ M	11 $\beta$ -HSD1 % activity at 20 $\mu$ M	11 $\beta$ -HSD1 IC <sub>50</sub> ( $\mu$ M)
26	84 $\pm$ 13	n.d.	59 $\pm$ 5	96 $\pm$ 4	not inhibited	110 $\pm$ 10	n.d.
27	76 $\pm$ 9	n.d.	48 $\pm$ 3	89 $\pm$ 11	not inhibited	106 $\pm$ 9	n.d.
28	88 $\pm$ 12	n.d.	55 $\pm$ 8	95 $\pm$ 5	not inhibited	68 $\pm$ 5	n.d.
29	16 $\pm$ 6	5.7 $\pm$ 1	76 $\pm$ 4	96 $\pm$ 8	not inhibited	70 $\pm$ 4	> 50
30	75 $\pm$ 11	n.d.	76 $\pm$ 2	80 $\pm$ 3	not inhibited	56 $\pm$ 4	n.d.
31	34 $\pm$ 6	33 $\pm$ 9	63 $\pm$ 6	75 $\pm$ 5	not inhibited	81 $\pm$ 4	n.d.
32	73 $\pm$ 9	n.d.	113 $\pm$ 17	76 $\pm$ 7	not inhibited	90 $\pm$ 5	n.d.
33	70 $\pm$ 14	n.d.	105 $\pm$ 2	19 $\pm$ 2	not inhibited	16 $\pm$ 2	6.2 $\pm$ 1.1
34	64 $\pm$ 7	n.d.	56 $\pm$ 5	92 $\pm$ 4	not inhibited	101 $\pm$ 6	n.d.
35	74 $\pm$ 2	n.d.	90 $\pm$ 12	57 $\pm$ 6	not inhibited	36 $\pm$ 4	20 $\pm$ 4
36	90 $\pm$ 9	n.d.	79 $\pm$ 2	86 $\pm$ 11	84 $\pm$ 5	87 $\pm$ 8	n.d.
37	63 $\pm$ 8	47 $\pm$ 10	97 $\pm$ 19	69 $\pm$ 5	45 $\pm$ 7	9 $\pm$ 2	3.8 $\pm$ 1.2
38	84 $\pm$ 9	n.d.	59 $\pm$ 7	99 $\pm$ 9	not inhibited	99 $\pm$ 5	n.d.
39	54 $\pm$ 3	19 $\pm$ 4	86 $\pm$ 6	55 $\pm$ 7	not inhibited	96 $\pm$ 6	n.d.

<sup>a</sup> 11 $\beta$ -HSD activities and 17 $\beta$ -HSD1 and 17 $\beta$ -HSD2 activities were measured in lysates of HEK-293 cells expressing recombinant human enzymes as described previously.<sup>42,61</sup> For 17 $\beta$ -HSD3 and 17 $\beta$ -HSD5, the conversion of androstenedione to testosterone was measured in intact cells without adding exogenous cofactor.

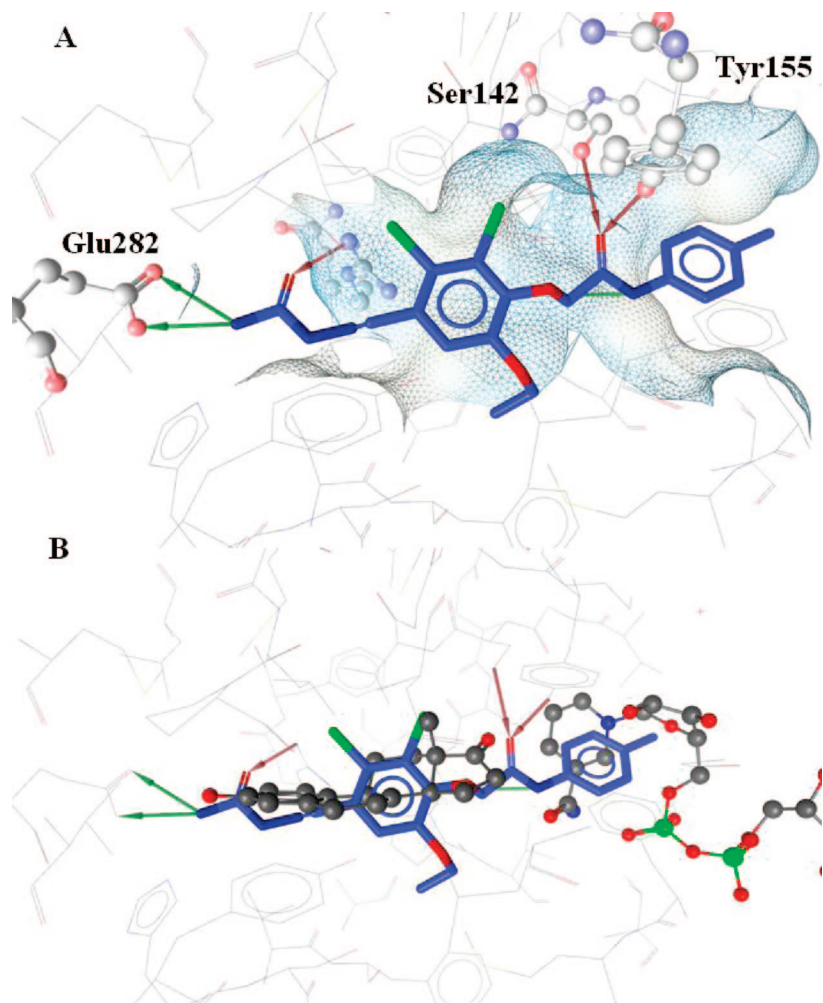


**Figure 5.** (A) Compound **29** docked into the ligand binding site of 17 $\beta$ -HSD1. Crucial hydrogen bonds are highlighted (red arrows, hydrogen bond acceptors; green arrows, hydrogen bond donors). (B) Compound **29** occupies the substrate binding site as well as parts of the cofactor binding site. The inhibitor in the active site (equilin) and the cofactor NADP are colored in dark gray and depicted in ball-and-stick style.

applied a recently constructed 11 $\beta$ -HSD1 pharmacophore<sup>42</sup> and investigated whether small substituents tolerated but not favorable in comparison to estrone pharmacophore models were able to predict the newly identified inhibitors as actives. Screening of compounds **33**, **35**, and **37** against the original restrictive 11 $\beta$ -HSD1 model resulted in retrieving compound **33** as a hit. When the shape restriction of the model was deleted, also compound **37** was correctly predicted as active (Supporting

Information Figure S3). Compound **35** mapped well to most features of the original model; however, it was not able to fit the hydrogen bond donor and the hydrogen bond acceptor features concomitantly. In addition to pharmacophore feature mapping, the best fit values of the active compounds were compared to their in vitro activity. The best fit value of the more potent compound **37** (3.65) exceeded the one of compound **28** (2.80). These results point toward the use of nonrestrictive

pharmacophore models for the identification of nonselective SDR inhibitor scaffolds.

## Conclusions

The application of 17 $\beta$ -HSD1 pharmacophore models that were built on crystal structures containing steroidal ligands allowed rationalizing the experimentally determined inhibitory activities of a series of flavonoids. In silico screening of a virtual compound library using these 17 $\beta$ -HSD1 pharmacophores as search queries led to the successful identification of novel nonsteroidal scaffolds that may serve as a basis for the development of more potent and selective 17 $\beta$ -HSD1 inhibitors. Moreover, we show that the use of pharmacophores of related SDR enzymes can facilitate the discrimination of selective against nonselective inhibitors, thereby improving the identification of specific 17 $\beta$ -HSD1 inhibitors. In future studies, small sublibraries of the identified inhibitors may be synthesized and tested again on different SDRs. These experiments should allow the identification of more potent and selective inhibitors as well as a further refinement of the pharmacophore models.

## Experimental Section

All calculations were performed on an AMD Athlon PC 1800+ CPU with 1 GB RAM running Windows 2000 and an equivalent Linux PC running Fedora Core 4, respectively.

**Structure-Based Pharmacophore Modeling.** Pharmacophore models were generated with LigandScout 2.0.<sup>48,49</sup> LigandScout is a software tool for generating 3D pharmacophores from structural data of macromolecular complexes (e.g., X-ray crystal structures). For model generation, all possible interactions between the ligand and the protein are considered. Chemical features are placed on the small molecule ligand according to predefined distances, geometry constraints, and potential interaction partners from the macromolecule, e.g., a protein. The automatically generated model can be manually refined by the user and exported in data formats readable by other modeling software (e.g., phase,<sup>65</sup> MOE, Catalyst). For the final models in our work, only essential interactions with the enzyme were kept. The models were imported into Catalyst 4.11 via the hypoedit tool.<sup>50</sup> Multiple features were reduced and hydrophobic features were shifted on the steroidal scaffold where Catalyst software would have placed them. The final models were validated with test sets and used for database screening. Additionally, in order to determine whether the model identifies a high number of random compounds as actives, a search in the WDI version 2003 was conducted using fast flexible search. The WDI is a database containing 63307 approved drugs and biologically active compounds. For a subset of the WDI, data on the compound's mode of action (e.g., antiestrogen) or activity keywords (e.g., virucide) are included.

**Docking.** For a further verification of hits, interesting testing candidates were docked into the active site of 17 $\beta$ -HSD1 (PDB entry 1equ). The ligand and the cofactor were excised from the macromolecule environment and hydrogens were added to the target using the Sybyl 7.1 Biopolymer module.<sup>66</sup> For the ligands, a standard 3D geometry was generated by Corina 3.00.<sup>67</sup> Subsequently, these conformers were minimized using Omega 2.0.<sup>68</sup> Both programs were run using default settings with special attention on the preservation of stereochemical information. For docking, GOLD 3.0.1 was used. All water molecules from the active site were toggled on/off, and the respective water orientation was set to "spin" as described.<sup>69,42</sup> In a first step, the performance of GOLD was analyzed by redocking of equilin into the binding pocket of the pdb entry 1equ with several different genetic algorithm setups. The binding site was defined as a 10 Å sphere around the centroid coordinates of equilin. After initial tests, the number of genetic algorithm runs was set to 5 and early termination was allowed if the top three solutions were within 1.5 Å rmsd. A template similarity constraint based on the shape of equilin showed favorable effects

on the generated docking poses. Because we found that using the 7–8 times speed up option does not significantly lower the quality of the calculated docking poses, we used this speed-optimized approach for further investigations. The ChemScore function showed appropriate scoring performance. The derived docking positions were visually inspected and evaluated according to their predicted binding position and interactions with the enzyme.

**Enzyme Activity Assay.** For determination of enzyme activity, HEK-293 cells were transfected by the calcium phosphate precipitation method with expression plasmids for human 17 $\beta$ -HSD or 11 $\beta$ -HSD enzymes, respectively. Cells were harvested 48 h post-transfection, washed with phosphate buffered saline, and centrifuged for 4 min at 150g. Supernatants were removed, cell pellets quick-frozen in a dry ice–ethanol bath, and stored at –70 °C. For measuring 17 $\beta$ -HSD1 reductase activity, cell pellets were suspended in a buffer containing 50 mM potassium phosphate, 20% glycerol, and 1 mM EDTA, followed by immediate determination of the conversion of 200 nM radiolabeled estrone to estradiol in the presence of 500  $\mu$ M cofactor NADPH. The conversion of androstenedione to testosterone by 17 $\beta$ -HSD3 and 17 $\beta$ -HSD5 was measured in the absence of exogenous cofactor in intact cells. 17 $\beta$ -HSD2 activity was assessed by incubating cell lysates in buffer containing 200 nM radiolabeled estradiol and 500  $\mu$ M cofactor NAD<sup>+</sup> as described previously.<sup>61</sup> The 11 $\beta$ -HSD1-dependent conversion of cortisone to cortisol in the presence of NADPH was measured as described earlier.<sup>70</sup> Inhibitors were diluted from stock solutions in DMSO and immediately used for activity assays. The DMSO concentration did not exceed 0.1% and had no effect on enzyme activities. No cytotoxicity was observed in MTT assays at the concentrations used in the present study. Data (mean  $\pm$  SD) were obtained from three independent experiments and were calculated using the Data Analysis Toolbox (Elsevier MDL, Allschwil, Switzerland).

**Acknowledgment.** We thank Dr. R emy Hoffmann, Accelrys, for performing the searches in the WDI. We thank Andreas Furer for technical support. This study was supported by grants from the Swiss National Science Foundation (no. 310000-112279 to A.O.) and the Swiss Cancer League (no. OCS-01402-08-2003 to A.O.). A.O. is a Novartis Research Foundation Professor.

**Supporting Information Available:** A list of PDB entries for 17 $\beta$ -HSD1 is given in Table S1. Table S2 describes structure–activity relationships of steroidal 17 $\beta$ -HSD1 inhibitors. Additional figures from the Supporting Information comprise the steric clash of hesperitin as observed in pharmacophore-based docking, compound **4** fitted to the 1 $\beta$ r-reduced model, and compound **37** fitted to pharmacophore models from 17 $\beta$ -HSD1 as well as 11 $\beta$ -HSD1. This material is available free of charge via the Internet at <http://pubs.acs.org>.

## References

- (1) Moeller, G.; Adamski, J. Multifunctionality of human 17 $\beta$ -hydroxysteroid dehydrogenases. *Mol. Cell. Endocrinol.* **2006**, *248*, 47–55.
- (2) Adamski, J.; Jakob, F. J. A guide to 17 $\beta$ -hydroxysteroid dehydrogenases. *Mol. Cell. Endocrinol.* **2001**, *171*, 1–4.
- (3) Mindnich, R.; M oller, G.; Adamski, J. The role of 17 $\beta$ -hydroxysteroid dehydrogenases. *Mol. Cell. Endocrinol.* **2004**, *218*, 7–20.
- (4) Lukacik, P.; Keller, B.; Bunkoczi, G.; Kavanagh, K. L.; Lee, W. H.; Adamski, J.; Oppermann, U. Structural and biochemical characterization of human orphan DHRS10 reveals a novel cytosolic enzyme with steroid dehydrogenase activity. *Biochem. J.* **2007**, *204*, 419–427.
- (5) Luu-The, V. Analysis and characteristics of multiple types of human 17 $\beta$ -hydroxysteroid dehydrogenase. *J. Steroid Biochem. Mol. Biol.* **2001**, *76*, 143–151.
- (6) Poirier, D. Inhibitors of 17 $\beta$ -hydroxysteroid dehydrogenases. *Curr. Med. Chem.* **2003**, *10*, 453–477.
- (7) Neumann, F.; Schenck, B.; Schleusener, H.; Schweikert, H. U., Endokrinpharmakologie. In *Allgemeine und Spezielle Pharmakologie und Toxikologie*; Forth, W., Henschler, D., Rummel, W., Starke, K., Eds.; Spektrum Verlag: M unchen, 1992.

- (8) Labrie, F.; Simard, J.; Luu-The, V.; Pelletier, G.; Belghmi, K.; Belanger, A. Structure, regulation and role of  $3\beta$ -hydroxysteroid dehydrogenase,  $17\beta$ -hydroxysteroid dehydrogenase and aromatase enzymes in the formation of sex steroids in classical and peripheral intracrine tissues. *Bailliere's Clin. Endocrinol. Metab.* **1994**, *8*, 451–474.
- (9) Gunnarsson, C.; Hellqvist, E.; Stal, O.  $17\beta$ -Hydroxysteroid dehydrogenases involved in local oestrogen synthesis have prognostic significance in breast cancer. *Br. J. Cancer* **2005**, *92*, 547–552.
- (10) Gunnarsson, C.; Jansson, A.; Holmlund, B.; Ferraud, L.; Nordenskjöld, B.; Rutqvist, L. E.; Skoog, L.; Stal, O. Expression of COX-2 and steroid converting enzymes in breast cancer. *Oncol. Rep.* **2006**, *16*, 219–224.
- (11) Oduwole, O. O.; Li, Y.; Isomaa, V. V.; Mäntyniemi, A.; Pulkka, A. E.; Soini, Y.; Vihko, P., T.  $17\beta$ -Hydroxysteroid dehydrogenase type 1 is an independent prognostic marker in breast cancer. *Cancer Res.* **2004**, *64*, 7604–7609.
- (12) Husen, B.; Huhtinen, K.; Poutanen, M.; Kangas, L.; Messinger, J.; Thole, H. Evaluation of inhibitors for  $17\beta$ -hydroxysteroid dehydrogenase type 1 in vivo in immunodeficient mice inoculated with MCF-7 cells stably expressing the recombinant human enzyme. *Mol. Cell. Endocrinol.* **2006**, *248*, 109–113.
- (13) Oduwole, O. O.; Mäkinen, M. J.; Isomaa, V. V.; Pulkka, A. E.; Jernvall, P.; Karttunen, T. J.; Vihko, P., T.  $17\beta$ -hydroxysteroid dehydrogenase type 2: independent prognostic significance and evidence of estrogen protection in female patients with colon cancer. *J. Steroid Biochem. Mol. Biol.* **2003**, *87*, 133–140.
- (14) Vihko, P.; Isomaa, V.; Ghosh, D. Structure and function of  $17\beta$ -hydroxysteroid dehydrogenase type 1 and type 2. *Mol. Cell. Endocrinol.* **2001**, *171*, 71–76.
- (15) Breton, R.; Housset, D.; Mazza, C.; Fontecilla Camps, J. C. The structure of a complex of human  $17\beta$ -hydroxysteroid dehydrogenase with estradiol and NADP<sup>+</sup> identifies two principal targets for the design of inhibitors. *Structure* **1996**, *4*, 905–915.
- (16) Berman, H. M.; Westbrook, J.; Feng, Z.; Gililand, G.; Bhat, T. N.; Weissig, H.; Shindyalov, I. N.; Bourne, P. E. The Protein Data Bank. *Nucleic Acids Res.* **2000**, *28*, 235–242.
- (17) Ghosh, D.; Pletnev, V. Z.; Zhu, D.-W.; Wawrzak, Z.; Duax, W. L.; Pangborn, W.; Labrie, F.; Lin, S.-X. Structure of human estrogenic  $17\beta$ -hydroxysteroid dehydrogenase at 2.20 Å resolution. *Structure* **1995**, *3*, 503–513.
- (18) Han, Q.; Campbell, R. L.; Gangloff, A.; Huang, Y.-W.; Lin, S.-X. Dehydroepiandrosterone and dihydrotestosterone recognition by human estrogenic  $17\beta$ -hydroxysteroid dehydrogenase: C-18/C-19 steroid discrimination and enzyme-induced strain. *J. Biol. Chem.* **2000**, *275*, 1105–1111.
- (19) Sawicki, M. W.; Erman, M.; Puranen, T.; Vihko, P.; Ghosh, D. Structure of the ternary complex of human  $17\beta$ -hydroxysteroid dehydrogenase type 1 with 3-hydroxyestra-1,3,5,7-tetraen-17-one (equilin) and NADP<sup>+</sup>. *Proc. Natl. Acad. Sci. U.S.A.* **1999**, *96*, 840–845.
- (20) Mazza, C.; Breton, R.; Housset, D.; Fontecilla-Camps, J. C. Unusual charge stabilization of NADP<sup>+</sup> in  $17\beta$ -hydroxysteroid dehydrogenase. *J. Biol. Chem.* **1998**, *273*, 8145–8152.
- (21) Qiu, W.; Campbell, R. L.; Gangloff, A.; Dupuis, P.; Boivin, R. P.; Tremblay, M. R.; Poirier, D.; Lin, S.-X. A concerted, rational design of type 1  $17\beta$ -hydroxysteroid dehydrogenase inhibitors: estradiol-adenosine hybrids with high affinity. *FASEB J.* **2002**, *16*, 1829–1831.
- (22) Azzi, A.; Rehse, P. H.; Zhu, D.-W.; Campbell, R. L.; Labrie, F.; Lin, S.-X. Crystal structure of human estrogenic  $17\beta$ -hydroxysteroid dehydrogenase complexed with  $17\beta$ -estradiol. *Nat. Struct. Biol.* **1996**, *3*, 665–668.
- (23) Gangloff, A.; Shi, R.; Nahoum, V.; Lin, S.-X. Pseudo-symmetry of C19 steroids, alternative binding orientations, and multispecificity in human estrogenic  $17\beta$ -hydroxysteroid dehydrogenase. *FASEB J.* **2003**, *17*, 274–276.
- (24) Shi, R.; Lin, S.-X. Cofactor Hydrogen Bonding onto the Protein Main Chain Is Conserved in the Short Chain Dehydrogenase/Reductase Family and Contributes to Nicotinamide Orientation. *J. Biol. Chem.* **2004**, *279*, 16778–16785.
- (25) Brown, W. M.; Metzger, L. E.; Barlow, J. P.; Hunsaker, L. A.; Deck, L. M.; Royer, R. E.; Vander Jagt, D. L.  $17\beta$ -Hydroxysteroid dehydrogenase type 1: computational design of active site inhibitors targeted to the Rossmann fold. *Chem. Biol. Interact.* **2003**, *143*–144, 481–491.
- (26) Allan, G. M.; Bubert, C.; Vicker, N.; Smith, A.; Tutill, H. J.; Purohit, A.; Reed, M. J.; Potter, B. V. L. Novel, potent inhibitors of  $17\beta$ -hydroxysteroid dehydrogenase type 1. *Mol. Cell. Endocrinol.* **2006**, *248*, 204–207.
- (27) Allan, G. M.; Lawrence, H. R.; Cornet, J.; Bubert, C.; Fischer, D. S.; Vicker, N.; Smith, A.; Tutill, H. J.; Purohit, A.; Day, J. M.; Mahon, M. F.; Reed, M. J.; Potter, B. V. L. Modification of estrone at the 6, 16, and 17 positions: novel potent inhibitors of  $17\beta$ -hydroxysteroid dehydrogenase type 1. *J. Med. Chem.* **2006**, *49*, 1325–1345.
- (28) Poirier, D.; Dionne, P.; Auger, S. A  $6\beta$ -(thiaheptanamide) derivative of estradiol as inhibitor of  $17\beta$ -hydroxysteroid dehydrogenase type 1. *J. Steroid Biochem. Mol. Biol.* **1998**, *64*, 83–90.
- (29) Pelletier, J. D.; Poirier, D. Synthesis and evaluation of estradiol derivatives with  $16\alpha$ -(bromoalkylamide),  $16\alpha$ -(bromoalkyl), or  $16\alpha$ -(bromoalkynyl) side chain as inhibitors of  $17\beta$ -hydroxy steroid dehydrogenase type 1 without estrogenic activity. *Bioorg. Med. Chem.* **1996**, *4*, 1617–1628.
- (30) Sam, K.-M.; Boivin, R. P.; Tremblay, M. R.; Auger, S.; Poirier, D. C16 and C17 derivatives of estradiol as inhibitors of  $17\beta$ -hydroxysteroid dehydrogenase type 1: chemical synthesis and structure-activity relationships. *Drug Des. Discovery* **1998**, *15*, 157–180.
- (31) Owen, C. P.; Ahmed, S. The derivation of a potential transition state for the reduction reaction catalyzed by  $17\beta$ -hydroxysteroid dehydrogenase—an approximate representation of its active site for use in drug design and discovery. *Biochem. Biophys. Res. Commun.* **2004**, *318*, 131–134.
- (32) Deluca, D.; Möller, G.; Rosinus, A.; Elger, W.; Hillisch, A.; Adamski, J. Inhibitory effects of fluorine-substituted estrogens on the activity of  $17\beta$ -hydroxysteroid dehydrogenases. *Mol. Cell. Endocrinol.* **2006**, *248*, 218–224.
- (33) Fischer, D. S.; Allan, G. M.; Bubert, C.; Vicker, N.; Smith, A.; Tutill, H. J.; Purohit, A.; Wood, L.; Packham, G.; Mahon, M. F.; Reed, M. J.; Potter, B. V. L. E-ring modified steroids as novel potent inhibitors of  $17\beta$ -hydroxysteroid dehydrogenase type 1. *J. Med. Chem.* **2005**, *48*, 5749–5770.
- (34) Poirier, D.; Chang, H.-J.; Azzi, A.; Boivin, R. P.; Lin, S.-X. Estrone and estradiol C-16 derivatives as inhibitors of type 1  $17\beta$ -hydroxysteroid dehydrogenase. *Mol. Cell. Endocrinol.* **2006**, *248*, 236–238.
- (35) Lawrence, H. R.; Vicker, N.; Allan, G. M.; Smith, A.; Mahon, M. F.; Tutill, H. J.; Purohit, A.; Reed, M. J.; Potter, B. V. L. Novel and potent  $17\beta$ -hydroxysteroid dehydrogenase type 1 inhibitors. *J. Med. Chem.* **2005**, *48*, 2759–2762.
- (36) Bérubé, M.; Poirier, D. Synthesis of simplified hybrid inhibitors of type 1  $17\beta$ -hydroxysteroid dehydrogenase via cross-metathesis and Sonogashira coupling reactions. *Org. Lett.* **2004**, *6*, 3127–3130.
- (37) Messinger, J.; Hirvelä, L.; Husen, B.; Kangas, L.; Koskimies, P.; Pentikäinen, O.; Pauli, S.; Thole, H. New inhibitors of  $17\beta$ -hydroxysteroid dehydrogenase type 1. *Mol. Cell. Endocrinol.* **2006**, *248*, 192–198.
- (38) Krazeisen, A.; Breitling, R.; Moeller, G.; Adamski, J. Phytoestrogens inhibit human  $17\beta$ -hydroxysteroid dehydrogenase type 5. *Mol. Cell. Endocrinol.* **2001**, *171*, 151–162.
- (39) Schweizer, R. A.; Atanasov, A. G.; Frey, B. M.; Odermatt, A. A rapid screening assay for inhibitors of  $11\beta$ -hydroxysteroid dehydrogenases ( $11\beta$ -HSD): flavanone selectively inhibits  $11\beta$ -HSD1 reductase activity. *Mol. Cell. Endocrinol.* **2003**, *212*, 41–49.
- (40) Krazeisen, A.; Breitling, R.; Möller, G.; Adamski, J. Human  $17\beta$ -hydroxysteroid dehydrogenase type 5 is inhibited by dietary flavonoids. *Adv. Exp. Med. Biol.* **2002**, *505*, 151–161.
- (41) Langer, T.; Hoffmann, R. D., *Pharmacophores and Pharmacophore Searches*; Wiley-VCH: Weinheim, 2006; Vol. 32, p 375.
- (42) Schuster, D.; Maurer, E.; Laggner, C.; Nashev, L. G.; Wilckens, T.; Langer, T.; Odermatt, A. The discovery of new  $11\beta$ -hydroxysteroid dehydrogenase type I inhibitors by common feature pharmacophore modeling and virtual screening. *J. Med. Chem.* **2006**, *49*, 3454–3466.
- (43) Schuster, D.; Paluszczak, A.; Hartmann, R. W.; Langer, T. Pharmacophore modeling and in silico screening for cytochrome P450 19 (aromatase) inhibitors. *J. Chem. Inf. Model.* **2006**, *46*, 1301–1311.
- (44) Steindl, T. M.; Crump, C. E.; Hayden, F. G.; Langer, T. Pharmacophore modelling, docking, and principal component analysis-based clustering: combined computer-assisted approaches to identify new inhibitors of the human rhino virus coat protein. *J. Med. Chem.* **2005**, *48*, 6250–6260.
- (45) Rollinger, J. M.; Hornick, A.; Langer, T.; Stuppner, H.; Prast, H. Acetylcholinesterase inhibitory activity of scopolin and scopoletin discovered by virtual screening of natural products. *J. Med. Chem.* **2004**, *47*, 6248–6254.
- (46) Rollinger, J. M.; Bodensieck, A.; Seger, C.; Ellmerer, E. P.; Bauer, R.; Langer, T.; Stuppner, H. Discovering COX-inhibiting constituents of Morus root bark: activity-guided versus computer-aided methods. *Planta Med.* **2005**, *71*, 399–405.
- (47) Karkola, S.; Lilienkampff, A.; Wähälä, K. A 3D QSAR model of  $17\beta$ -HSD1 inhibitors based on a thieno[2,3-*d*]pyrimidin-4(3*H*)one core applying molecular dynamics simulations and ligand-protein docking. *ChemMedChem* **2008**, *3*, 461–472.



- (48) Wolber, G.; Langer, T. LigandScout: 3-D Pharmacophores Derived from Protein-Bound Ligands and Their Use as Virtual Screening Filters. *J. Chem. Inf. Comput. Sci.* **2005**, *45*, 160–169.
- (49) Wolber, G.; Dornhofer, A.; Langer, T. Efficient overlay of small molecules using 3-D pharmacophores. *J. Comput. Aided Mol. Des.* **2006**, *20*, 773–788.
- (50) *Catalyst Software Package, version 4.11*; Accelrys Software Inc.: San Diego, CA, 2005.
- (51) Alho-Richmond, S.; Lilienkampf, A.; Wähälä, K. Active site analysis of 17 $\beta$ -hydroxysteroid dehydrogenase type 1 enzyme complexes with SPROUT. *Mol. Cell. Endocrinol.* **2006**, *248*, 208–213.
- (52) Tremblay, M. R.; Lin, S.-X.; Poirier, D. Chemical synthesis of 16 $\beta$ -propylaminoacyl derivatives of estradiol and their inhibitory potency on type 1 17 $\beta$ -hydroxysteroid dehydrogenase and binding affinity on steroid receptors. *Steroids* **2001**, *66*, 821–831.
- (53) *Derwent World Drug Index, 2003*; Derwent Publications Ltd.: London, 2003.
- (54) Griffiths, K.; Morton, M. S.; Denis, L. Certain aspects of molecular endocrinology that relate to the influence of dietary factors on the pathogenesis of prostate cancer. *Eur. Urol.* **1999**, *35*, 443–455.
- (55) Ingram, D.; Sanders, K.; Kolybaba, M.; Lopez, D. Case-control study of phyto-oestrogens and breast cancer. *Lancet* **1997**, *350*, 990–994.
- (56) Morrissey, C.; Watson, R. W. Phytoestrogens and prostate cancer. *Curr. Drug Targets* **2003**, *4*, 231–241.
- (57) Whitehead, S. A.; Rice, S. Endocrine-disrupting chemicals as modulators of sex steroid synthesis. *Best Pract. Res. Clin. Endocrinol. Metab.* **2006**, *20*, 45–61.
- (58) Le Bail, J.-C.; Champavier, Y.; Chulia, A.-J.; Habrioux, G. Effects of phytoestrogens on aromatase, 3 $\beta$ - and 17 $\beta$ -hydroxysteroid dehydrogenase activities and human breast cancer cells. *Life Sci.* **2000**, *66*, 1281–1291.
- (59) Mäkälä, S.; Poutanen, M.; Kostian, M. L.; Lehtimäki, N.; Strauss, L.; Santti, R.; Vihko, R. Inhibition of 17 $\beta$ -hydroxysteroid oxidoreductase by flavonoids in breast and prostate cancer cells. *Proc. Soc. Exp. Biol. Med.* **1998**, *217*, 310–316.
- (60) Odermatt, A.; Arnold, P.; Stauffer, A.; Frey, B. M.; Frey, F. J. The N-terminal anchor sequences of 11 $\beta$ -hydroxysteroid dehydrogenases determine their orientation in the endoplasmic reticulum membrane. *J. Biol. Chem.* **1999**, *274*, 28762–28770.
- (61) Atanasov, A. G.; Nashev, L. G.; Tam, S.; Baker, M. E.; Odermatt, A. Organotins disrupt the 11 $\beta$ -hydroxysteroid dehydrogenase type 2-dependent local inactivation of glucocorticoids. *Environ. Health Perspect.* **2005**, *113*, 1600–1606.
- (62) Khan, N.; Sharma, K. K.; Andersson, S.; Auchus, R. J. Human 17 $\beta$ -hydroxysteroid dehydrogenases types 1, 2, and 3 catalyze bidirectional equilibrium reactions, rather than unidirectional metabolism, in HEK-293 cells. *Arch. Biochem. Biophys.* **2004**, *429*, 50–59.
- (63) Kristan, K.; Krajnc, K.; Konc, J.; Gobec, S.; Stojan, J.; Rizner, T. L. Phytoestrogens as inhibitors of fungal 17 $\beta$ -hydroxysteroid dehydrogenase. *Steroids* **2005**, *70*, 694–703.
- (64) Atanasov, A. G.; Odermatt, A. Readjusting the glucocorticoid balance: an opportunity for modulators of 11 $\beta$ -hydroxysteroid dehydrogenase type 1 activity. *Endocr. Metab. Immune Disord. Drug Targets* **2007**, *7*, 125–140.
- (65) Dixon, S. L.; Smondyrev, A. M.; Knoll, E. H.; Rao, S. N.; Shaw, D. E.; Friesner, R. A. PHASE: A new design for pharmacophore perception, 3D QSAR model development, and 3D database screening: 1. Methodology and preliminary results. *J. Comput. Aided Mol. Des.* **2006**, *20*, 647–671.
- (66) *Sybyl 7.1*; Tripos: St. Louis, MO, 2006.
- (67) *Corina Version 3.0*; Molecular Networks GmbH: Erlangen, Germany, 2003.
- (68) *Omega 2.0*; OpenEye Scientific Software: Santa Fe, NM, 2005.
- (69) *GOLD 3.1*; The Cambridge Crystallographic Data Centre—CCDC: Cambridge, 2004–2007.
- (70) Frick, C.; Atanasov, A. G.; Arnold, P.; Ozols, J.; Odermatt, A. Appropriate function of 11 $\beta$ -hydroxysteroid dehydrogenase type 1 in the endoplasmic reticulum lumen is dependent on its N-terminal region sharing similar topological determinants with 50 kDa esterase. *J. Biol. Chem.* **2004**, *279*, 31131–31138.

JM800054H